
IDENTIFICATION OF CRITICAL PARAMETERS FOR THE JOHNSON AND ETTINGER (1991) VAPOR INTRUSION MODEL

PAUL. C. JOHNSON
DEPARTMENT OF CIVIL AND ENVIRONMENTAL ENGINEERING, ARIZONA STATE UNIVERSITY

A SUMMARY OF RESEARCH RESULTS FROM API'S SOIL & GROUNDWATER TECHNICAL TASK FORCE

Executive Summary

At sites where soils or groundwater contain chemicals of concern, there is the potential for chemical vapors to migrate from the subsurface to nearby basements, buildings, and other enclosed spaces. The Johnson and Ettinger (1991) model and its extensions (e.g., API Publication 4674) are at this time the most widely used algorithms for assessing the intrusion of chemical vapors to enclosed spaces. To facilitate use of this model, the United States Environmental Protection Agency (USEPA) distributes Microsoft Excel™ spreadsheets and a comprehensive guidance document (USEPA 1997, 2000). These spreadsheet implementations of the model are user-friendly and have made the model more accessible; however, experience suggests that they have also made it easier to unknowingly use the model inappropriately. The spreadsheets require a large number of inputs, and as a result, relationships between model inputs and outputs are not well understood, many users are unable to identify the critical inputs, and this has contributed to confusion and disagreement concerning the utility of the model.

The objective of this work is to help users develop a better understanding of the relationships between model inputs and outputs so that they can identify critical inputs when applying the model. This is accomplished by first providing a brief overview of the Johnson and Ettinger (1991) model, including discussions distinguishing primary and secondary model inputs and the differences between the Johnson and Ettinger (1991) model and its implementation in the USEPA spreadsheets. Then, a flowchart-based approach for identifying critical model inputs is presented and reasonable ranges of model inputs are discussed. Finally, use of the flowchart approach is illustrated and compared with a more traditional sensitivity analysis. Appendix A presents the parametric analysis that is the basis for the flowchart-based approach.

1.0 Introduction

At sites where soils or groundwater contain chemicals of concern, there is the potential for chemical vapors to migrate from the subsurface to nearby basements, buildings, and other enclosed spaces as shown in Figure 1. In extreme cases, these vapors may accumulate at concentrations that pose near-term safety hazards (e.g., explosions or acute health effects) or aesthetic problems (i.e., odors); however, it is more likely that the chemical concentrations will be low, if detectable at all. In the case of lower concentrations the main concern is usually whether or not there is an unacceptable chance of longer-term chronic health effects.

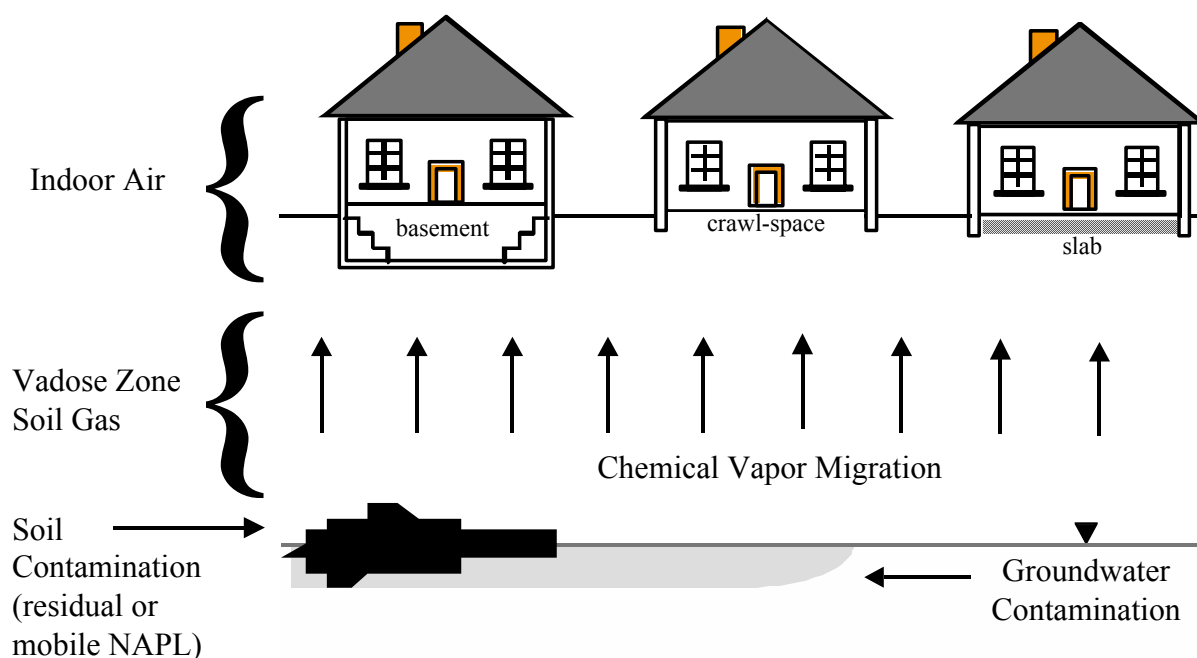


Figure 1. Generalized vapor migration-to-indoor-air schematic.

There are three basic options for identifying where this pathway is, and is not a concern. In the first approach, indoor air samples are collected and analyzed, and then the measured concentrations are compared with target indoor air concentrations. In the second approach, available experience and data are compiled and analyzed, and then empirical relationships between site conditions and expected impacts are developed. For example, one might use available data to derive empirical attenuation factors relating subsurface and indoor vapor concentrations, as is done for the Colorado Department of Transportation (CDOT) site in Johnson et al. (2002a). In the third approach, models that consider site conditions (geology, chemical concentrations in soils, vapors, and groundwater, etc.) are used to predict indoor air

concentrations. These three approaches need not be mutually exclusive, and each can play a role in some overall integrated framework for assessing potential vapor intrusion impacts (e.g., USEPA 2001).

Because many consider routine indoor air monitoring to be impracticable, and because data from only a few well-studied sites is available (e.g., Johnson et al. 2002a, Hers et al. 2001), the use of screening-level predictive algorithms has played an important role in assessing the significance of this pathway. For example, screening-level algorithms have been used to:

- estimate potential indoor impacts at specific sites,
- identify sites that require further assessment,
- develop chemical- and media-specific target concentrations (e.g., look-up tables) for identifying settings that are of concern, and
- identify how site-specific indoor air concentrations or target soil and groundwater concentrations are expected to change with changes in site and chemical characteristics

The Johnson and Ettinger (1991) algorithm and its extensions (e.g., Johnson et al. 1998, Johnson et al. 1999) are the most widely used at this time. To facilitate use of the Johnson and Ettinger (1991) model, the United States Environmental Protection Agency (USEPA) distributes Microsoft Excel™ spreadsheets and a comprehensive guidance document (USEPA 1997, 2000). These products are user-friendly and have made the model more accessible; however, experience suggests that they have also made it easier for many to unknowingly use the model inappropriately. The spreadsheets require a large number of inputs, and as a result, relationships between model inputs and outputs are not well understood, many users are unable to identify the critical inputs, and this has contributed to confusion and disagreement concerning the utility of the model. The following may also be contributors:

- the USEPA spreadsheets couple other calculations to the Johnson and Ettinger (1991) algorithm,
- most of the Johnson and Ettinger (1991) model inputs are not collected during a typical site characterization, and therefore, they have to be estimated or inferred from available data and other non-site-specific sources of information, and
- many believe the Johnson and Ettinger (1991) model output to be very sensitive to uncertainties in model inputs, and therefore feel that the model is of little use until all inputs are known with precision on a site-specific basis.

The objective of this work is to help users develop a better understanding of the relationships between model inputs and outputs so that they can identify critical inputs when applying the model. This is accomplished by first providing a brief overview of the Johnson and Ettinger (1991) model, including discussions distinguishing primary and secondary model inputs and the differences between the Johnson and Ettinger (1991) model and its implementation in the USEPA spreadsheets. Then, a flowchart-based approach for identifying critical model inputs is presented and reasonable ranges of model inputs are discussed. Finally, use of the flowchart approach is illustrated and compared with a more traditional sensitivity analysis. Appendix A presents the parametric analysis that is the basis for the flowchart-based approach.

It should be noted that this document only addresses use of the Johnson and Ettinger (1991) model, and this version does not account for biodegradation in the vadose zone. Thus the sensitivity of model results to parameters characterizing biodegradation is not addressed in this document. This issue is addressed in Johnson et al. (1998), Johnson et al. (1999), and Johnson et al. (2002b). In brief, inclusion of biodegradation will result in smaller attenuation factors and decreased indoor air concentrations relative to the case with no biodegradation. Johnson et al. (1998) and Johnson et al. (1999) show that the calculations can be extremely sensitive to first-order rate constant changes, when biodegradation is modeled as a simple first order reaction process. In Johnson et al. (2002b), oxygen-limited first-order biodegradation is modeled and those model results are also sensitive to small changes in first-order rate constants.

2.0 Overview of the Johnson and Ettinger (1991) Model and Its USEPA Spreadsheet Implementation

A brief introduction to the Johnson and Ettinger (1991) algorithm is provided below. The concept of “primary” and “secondary” inputs is introduced and differences between the Johnson and Ettinger (1991) model and its implementation by USEPA in Microsoft Excel™ spreadsheets (1997 – 2001) are identified.

2.1 The Johnson and Ettinger (1991) Algorithm

Screening level algorithms for the vapor intrusion pathway (Johnson and Ettinger 1991, Little et al. 1992, Johnson et al. 1998) couple source zone partitioning, vadose zone transport, building foundation transport, and enclosed-space mixing equations. The resulting algorithms then depend on inputs related to soil, chemical, and building characteristics. The output of the Johnson and Ettinger (1991) algorithm is an estimate of the “vapor attenuation coefficient”

α [dimensionless]. This quantity represents the ratio of the indoor vapor concentration C_{indoor} to the vapor concentration C_{source} found at some depth L_T below a foundation:

$$\alpha = \frac{\left[\frac{D_T^{\text{eff}} A_B}{Q_B L_T} \right] \exp\left(\frac{Q_{\text{soil}} L_{\text{crack}}}{D_{\text{crack}}^{\text{eff}} \eta A_B} \right)}{\exp\left(\frac{Q_{\text{soil}} L_{\text{crack}}}{D_{\text{crack}}^{\text{eff}} \eta A_B} \right) + \left[\frac{D_T^{\text{eff}} A_B}{Q_B L_T} \right] + \left[\frac{D_T^{\text{eff}} A_B}{Q_{\text{soil}} L_T} \right] \left(\exp\left(\frac{Q_{\text{soil}} L_{\text{crack}}}{D_{\text{crack}}^{\text{eff}} \eta A_B} \right) - 1 \right)} \quad (1)$$

where $\alpha = (C_{\text{indoor}}/C_{\text{source}})$, and:

- A_B = the surface area of the enclosed space in contact with soil [m^2]
- $D_{\text{crack}}^{\text{eff}}$ = the effective overall vapor-phase diffusion coefficient through the walls and foundation cracks [m^2/d]
- D_T^{eff} = the effective overall vapor-phase diffusion coefficient in soil between the foundation and the depth L_T [m^2/d]
- L_{crack} = the enclosed space foundation thickness [m]
- L_T = the distance (depth) to the vapor source or other point of interest below foundation [m], measured from the foundation to the vapor source or other point of interest
- Q_B = the enclosed space volumetric air flow rate [m^3/d] of fresh air; usually estimated to be the product of the enclosed-space volume (V_B [m^3]) and the indoor air exchange rate with outdoor air (E_B [1/d])
- Q_{soil} = the pressure-driven soil gas flow rate from the subsurface into the enclosed space [m^3/d]
- η = the fraction of enclosed space surface area open for vapor intrusion [m^2/m^2]; this is sometimes referred to as the “crack factor” and is estimated to be the total area of cracks, seams, and any perforations of surfaces in contact with soil divided by the total area in contact with soil.

Figure 2 presents the conceptual basis for this algorithm; it also displays the relationship between the eight primary model inputs and the processes and system components that they characterize.

It should be noted that Equation (1) is the steady-source version of this algorithm. A depleting source form of this equation is also presented in Johnson and Ettinger (1991); however, this document focuses on the steady-source version as it is the most widely used in practice. The use of a steady source term implies an infinite source mass since the chemical concentration at the source never decreases. When the model is to be used for long-term estimation, it is appropriate to perform a reality check by comparing the calculated flux rate with the estimated mass available for volatilization to see if the volatilization rate is sustainable for a reasonable length of time (Johnson et al. 1991, equation 27).

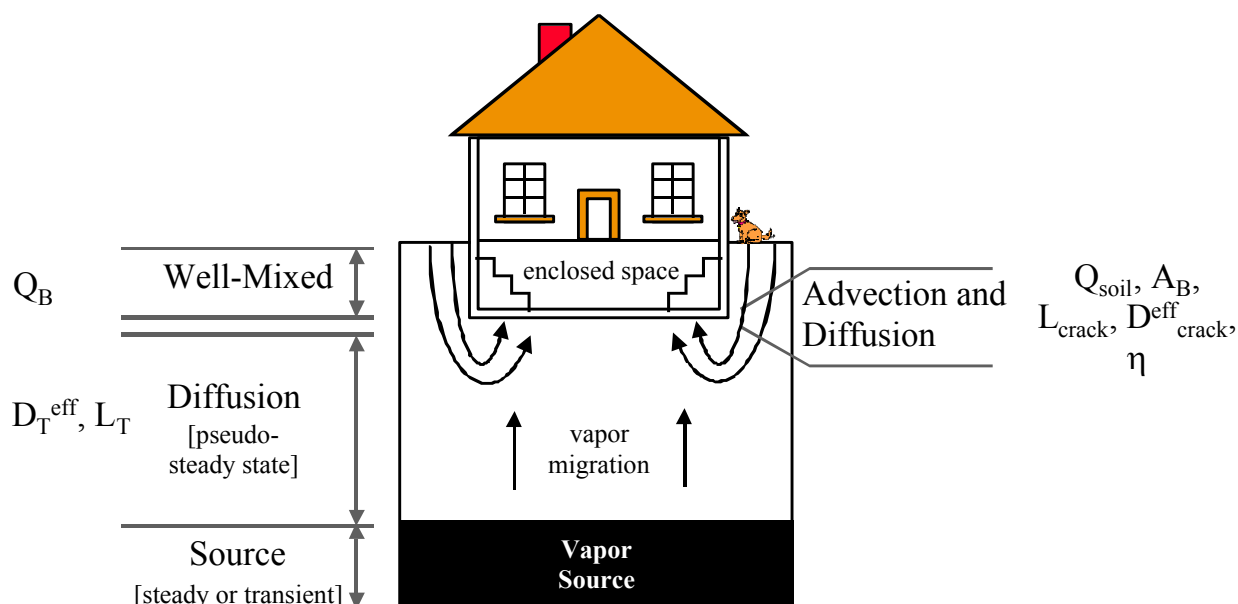


Figure 2. Johnson and Ettinger (1991) conceptual model showing the primary model inputs and the processes and system components that they characterize.

2.2 Primary and Secondary Model Inputs

Eight “primary” inputs appear in Equation (1) (D_T^{eff} , $D_{\text{crack}}^{\text{eff}}$, Q_{soil} , Q_B , A_B , η , L_{crack} , L_T). Of these, only L_T is likely to be obtained from typical site characterization data. Two others – A_B and L_{crack} – might easily be measured or at least reasonably estimated based on visual

observation or experience. The remaining inputs (D_T^{eff} , $D_{\text{crack}}^{\text{eff}}$, Q_{soil} , Q_B , and η) must be estimated from knowledge of reasonable ranges for their values, or from expressions relating them to “secondary” inputs that are presumably known.

The effective porous media overall vapor-phase diffusion coefficients (D_T^{eff} , $D_{\text{crack}}^{\text{eff}}$) are generally determined from a combination of partitioning expressions and the Millington-Quirk effective diffusion coefficient formulation (Millington 1959, Millington and Quirk 1961, Millington and Shearer 1971, Johnson and Ettinger 1991):

$$D^{\text{eff}} = D^{\text{air}} \frac{\theta_v^{3.33}}{\theta_T^2} + \left(\frac{D^{\text{H}_2\text{O}}}{H_i} \right) \frac{\theta_m^{3.33}}{\theta_T^2} \quad (2)$$

where:

- H_i = the chemical-specific Henry's Law constant [(ug/m³-vapor)/(ug/m³-H₂O)]
- θ_m = the volumetric moisture content [m³-H₂O/m³-soil]
- θ_T = the total porosity [m³-voids/m³-soil]
- θ_v = the volumetric vapor content (= $\theta_T - \theta_m$) [m³-vapor/m³-soil]
- D^{air} = the chemical-specific molecular diffusion coefficient in air [m²/d]
- $D^{\text{H}_2\text{O}}$ = the chemical-specific molecular diffusion coefficient in water [m²/d]

$D_{\text{crack}}^{\text{eff}}$ is usually estimated using Equation (2) and assuming that the cracks are filled with soil of homogeneous porosity and moisture content. Calculation of D_T^{eff} may allow for layers of materials having different total porosities and moisture contents using the expression (Johnson et al. 1998, 1999):

$$\frac{D_T^{\text{eff}}}{L_T} = \frac{1}{\sum_{i=1}^n \left(\frac{L_i}{D_i^{\text{eff}}} \right)} \quad (3)$$

where the subsurface is divided into distinct strata, each having a thickness L_i [m] (L_T equals the sum of all layer thicknesses L_i) and an effective vapor-phase porous media diffusion coefficient

D_i^{eff} [m^2/d] calculated using Equation (2) and the layer-specific porosity and moisture content. For reference, the USEPA spreadsheets allow for three distinct layers. When modeling the flux from groundwater, the capillary zone diffusion resistance is incorporated through Equation 3 by treating the capillary zone as a separate layer.

The USEPA spreadsheets estimate Q_{soil} [m^3/s] using the following theoretical expression (Nazaroff 1992):

$$Q_{\text{soil}} = \frac{2 \pi k \Delta P X_{\text{crack}}}{\mu \ln(2 Z_{\text{crack}} / R_{\text{crack}})} \quad (4)$$

where:

- k = the soil permeability (near foundation) to air flow [m^2]
- ΔP = the indoor-outdoor pressure difference [$\text{g}/\text{m}\cdot\text{s}^2$]
- X_{crack} = the total length of cracks through which soil gas vapors are flowing [m]
- μ = the viscosity of air [$\text{g}/\text{m}\cdot\text{s}$]
- Z_{crack} = the crack opening depth below grade [m]
- R_{crack} = the effective crack radius or width ($=\eta A_B/X_{\text{crack}}$) [m]

This equation is based on the conceptualization that flow to a crack is similar to flow to a cylindrical sink placed at depth Z below grade. Therefore, the soil permeability should reflect the soil properties adjacent to the building.

In summary, this development started with the eight primary Johnson and Ettinger (1991) inputs. Most are not typically measured in a site characterization, and therefore empirical and theoretical expressions were introduced for $D_{\text{crack}}^{\text{eff}}$, D_T^{eff} , and Q_{soil} . In doing this, those three primary inputs were replaced by 12 secondary inputs (H_I , $[\theta_m, \theta_T]_{\text{soil}}$, $[\theta_m, \theta_T]_{\text{crack}}$, D^{air} , $D^{\text{H}_2\text{O}}$, k , ΔP , X_{crack} , μ , and Z_{crack}). If layered systems are modeled, then the model inputs again increase by three (L_i , θ_m , and θ_T) for each additional layer.

Therefore, the introduction of secondary inputs leads to a substantial increase in the total model inputs. This then makes it very difficult for users to correctly identify relationships between model inputs and output. For all practical purposes, this introduction of secondary

inputs increases the number of unknown inputs; of the new 12 (or more) secondary inputs, the chemical properties (H_i , D^{air} , $D^{\text{H}_2\text{O}}$, and μ) are known but the remaining eight (or more) secondary inputs are not normally measured accurately (if at all) in a typical site characterization.

2.3 Key Distinctions Between the Johnson and Ettinger (1991) Model and the USEPA (1997, 2000) Spreadsheet Implementation

Since it is not uncommon to have practitioners refer to the USEPA spreadsheets as “The Johnson and Ettinger Model”, it is useful to briefly point out a few key differences between the USEPA spreadsheet implementation and the original Johnson and Ettinger (1991) algorithm. These are summarized below in Table 1.

Table 1. Summary of Key Distinctions Between Johnson and Ettinger (1991) and Its USEPA Spreadsheet Implementation (1997, 2000).

Johnson and Ettinger (1991)	USEPA Spreadsheet Implementation (1997, 2000)
Output is α , the attenuation factor.	Outputs are the incremental risk level, hazard index, or target soil and groundwater cleanup concentrations for prescribed risk and hazard index. The attenuation factor α is an intermediate calculation not appearing on the final results page.
Q_{soil} , the pressure-driven soil gas entry flow rate is a user-defined primary input.	Q_{soil} , the pressure-driven soil gas entry flow rate is an intermediate calculation not appearing on the final results page; it is calculated from user inputs for soil permeability, pressure differential, perimeter crack length, etc..
Capillary zone moisture content and capillary zone thickness are user-defined.	Capillary zone moisture content and capillary zone thickness are assigned through built-in tables for UCS soil descriptors.
The calculation focuses on the ratio of the indoor vapor concentration to the soil gas concentration at some depth.	Soil-to-soil vapor partitioning relationships are introduced; initial spreadsheet implementation limited to single components where immiscible-phase contaminants are not present, although this is not clear to the user.
Common to both is the need to ensure reasonable inputs and consistency between inputs that are expected to be correlated with each other (e.g., total porosity and moisture content in the vadose zone).	

First, as stated in the introduction, the Johnson and Ettinger (1991) algorithm is used to estimate the vapor attenuation coefficient. Given the intended audience and their anticipated needs, the USEPA spreadsheets were designed so that the output focuses on predicted indoor air concentrations, incremental risks, hazard quotients, and target risk-based groundwater and soil clean-up levels. The vapor attenuation coefficient α is an intermediate calculation not appearing

on the final results page. The calculation of indoor air concentrations resulting from contaminated soils and groundwater adds vapor-soil and vapor-water partitioning expressions and related inputs. The quantification of potential adverse impacts and target clean-up levels necessitates the addition of expressions for estimating exposures and corresponding human health impacts.

The USEPA spreadsheets require input of many of the secondary inputs discussed above, and do not allow direct input of the primary inputs (D_T^{eff} , $D_{\text{crack}}^{\text{eff}}$, Q_{soil} , Q_B). The resulting primary inputs that are passed through to the α calculation appear only on an intermediate calculation page; based on the author's experience, these are not reviewed by most users. While the spreadsheets have built-in automatic checks for numerical errors, it is important to note that there are no built-in reasonableness checks. This is especially evident in the calculation of Q_{soil} , where there is the potential to input ranges of secondary inputs that produce unreasonable Q_{soil} estimates (i.e. $Q_{\text{soil}} \gg 10$ L/min). Also, users may input combinations of total porosity and moisture content that are not self-consistent or even reasonable for the soil type and hydrogeologic setting. Both of these issues are addressed further in Sections 3 and 4. In brief, it is recommended that the Johnson and Ettinger (1991) equation and the USEPA spreadsheets be reformulated so that the ratio (Q_{soil}/Q_B) is input instead of Q_{soil} and Q_B separately. Furthermore it is recommended that moisture saturations (volume of water/volume of pore space) be input rather than moisture content (mass of water/mass of soil). These quantities have reasonable bounds, and the author feels that use of them would decrease misapplication of the USEPA spreadsheets.

Some secondary input values are assigned automatically by the spreadsheets through built-in look-up tables, and are not user-defined. For example, capillary zone moisture content and capillary zone thickness are selected from a look-up table based on input of standard UCS soil descriptors. The user may enter the capillary zone total porosity, but it is not constrained to fall within reasonable values consistent with the other inputs selected by the spreadsheets for that soil type.

It is important to note here that the purpose of this discussion is not to discourage use of the USEPA spreadsheets. The USEPA spreadsheets calculate α values correctly using the resulting primary inputs, and many will find the spreadsheets to be user-friendly and well-suited for their needs. The purpose of this discussion is to alert users to these issues in the hope that they better understand that there are differences between the work of Johnson and Ettinger (1991) and the USEPA spreadsheets. It is also hoped that users that will review the intermediate

spreadsheet calculations (i.e., the primary inputs) to ensure reasonableness in the spreadsheet results.

3.0 A Generalized Approach for Identifying Critical Inputs and Assigning Reasonable Values of Inputs

There are eight primary Johnson and Ettinger (1991) model inputs; with the introduction of secondary inputs, a model application may involve 20 or more inputs. As a result, traditional methods (i.e., sequential variation of individual inputs and inspection of output) are of little use for developing an understanding of the relationships between individual inputs and model output, and for identifying critical model inputs.

Appendix A presents an alternate approach, based on a parametric analysis. This approach leads to the conclusion that model output depends only on three basic parameters. It also leads to the conclusion that the dependence of α on individual primary and secondary inputs can be deduced if one understands the relationships between these three parameters and α . The results of the parametric analysis are discussed below and are summarized in the flowchart presented in Figure 3.

3.1 The Three Key Parameters

As stated above, the analysis presented in Appendix A leads to the conclusion that model output depends only on three basic parameters:

$$A = \left[\frac{D_T^{\text{eff}}}{E_B \left(\frac{V_B}{A_B} \right) L_T} \right], \quad B = \left[\frac{\left(\frac{Q_{\text{soil}}}{Q_B} \right) E_B \left(\frac{V_B}{A_B} \right) L_{\text{crack}}}{D_{\text{crack}}^{\text{eff}} \eta} \right], \quad C = \left[\frac{Q_{\text{soil}}}{Q_B} \right] \quad (5)$$

Readers will note that the parameters A, B, and C appearing in Equation (5) are written in terms of (Q_{soil}/Q_B) , (V_B/A_B) , η , L_{crack} , L_T , D_T^{eff} , $D_{\text{crack}}^{\text{eff}}$, and E_B rather than Q_{soil} , Q_B , A_B , η , L_{crack} , L_T , D_T^{eff} , and $D_{\text{crack}}^{\text{eff}}$. This modified set of primary inputs is used because: a) reasonable values

for (V_B/A_B) and E_B are constrained to narrow ranges, b) use of the ratio (V_B/A_B) eliminates the possibility of users assigning inconsistent V_B and A_B values, c) use of the ratio (Q_{soil}/Q_B) eliminates the possibility of users assigning inconsistent Q_{soil} and Q_B values, and d) the literature provides more clues for selection of reasonable (Q_{soil}/Q_B) ratios than individual Q_{soil} values. The quantities E_B and V_B represent the enclosed-space air exchange rate [d^{-1}] and enclosed-space volume [m^3], and these are related to Q_B through the expression:

$$Q_B = V_B E_B \quad (6)$$

3.2 Generalized Flowchart Approach for Identifying Critical Inputs

A generalized flowchart-based approach for identifying critical and non-critical inputs is presented below in Figure 3. For the purposes of this discussion a “non-critical input” is one that can be varied without causing significant changes in the model output (e.g., less than a 20% variation in output across the likely range of values for that input). All other inputs are defined to be “critical inputs”. It is important to note, however, that use of the term “critical” in this context is not meant to imply that large changes in model output are caused by changes in the model inputs. In fact, changes in α are at most linear with changes in primary input values.

To use the flowchart, the user begins with reasonable estimates for the primary model inputs, and then calculates values for the parameters A, B, and C. Given these, the user then follows the relevant branch of the flowchart to the list of critical and non-critical primary inputs.

Readers will note that there are two branches of the Figure 3 flowchart for which all of the primary inputs are determined to be critical. In these cases, it may be useful to know that α is always bounded such that it will never exceed $\alpha=A$, as discussed in Appendix A. Thus, the number of critical primary inputs can be reduced from eight $\{(Q_{soil}/Q_B), (V_B/A_B), \eta, L_{crack}, L_T, D_T^{eff}, D_{crack}^{eff}, \text{ and } E_B\}$ to four $\{(V_B/A_B), L_T, D_T^{eff}, \text{ and } E_B\}$ if one is willing to accept a degree of conservatism in the estimated α values.

Use of this approach is illustrated in Section 5, where results of the flowchart-based approach are compared with results of a more traditional sensitivity analysis. Before doing that, however, it is important that reasonable ranges for the primary and secondary model inputs be discussed.

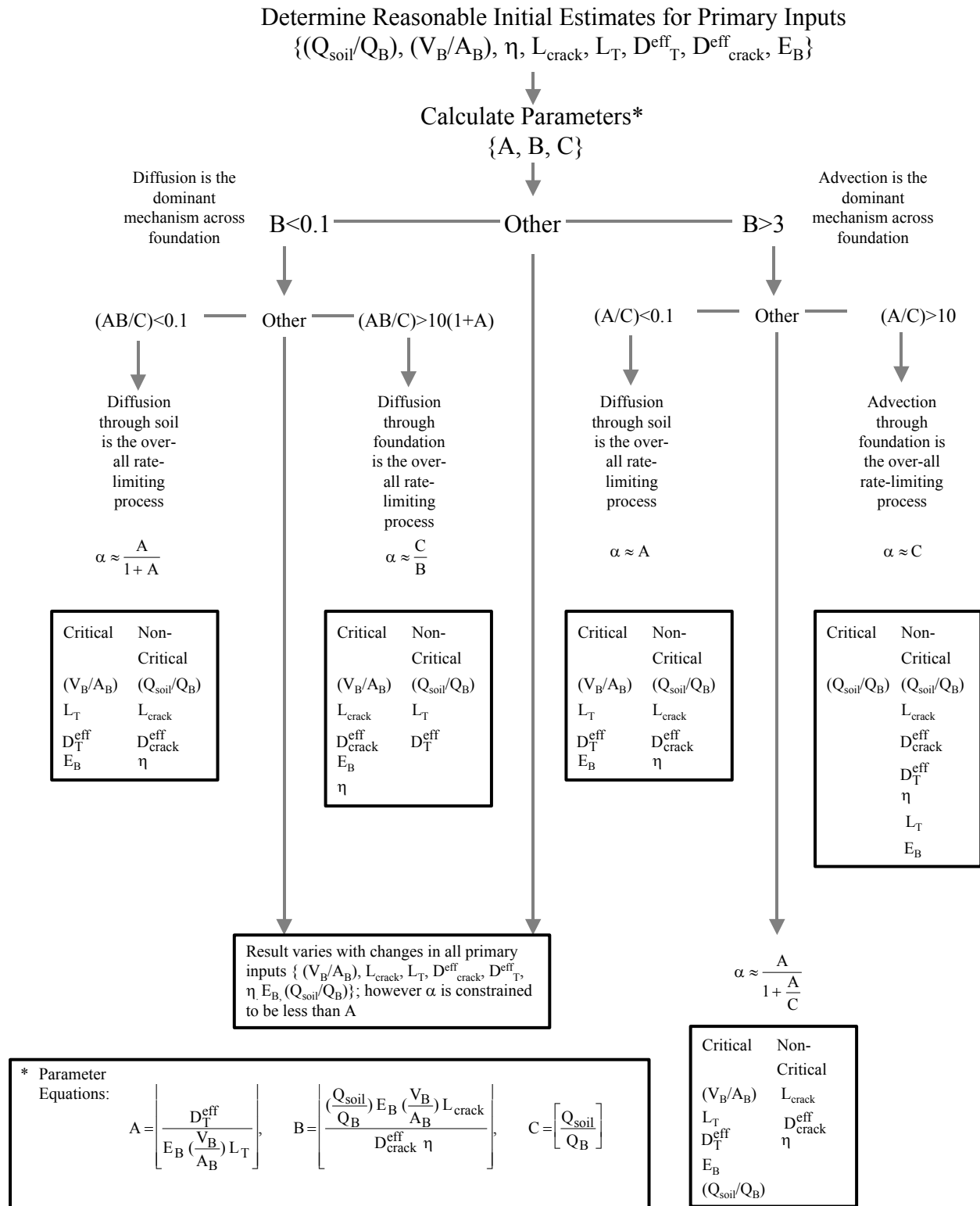


Figure 3. Generalized flowchart for identifying critical and non-critical parameters.

3.3 Johnson and Ettinger (1991) Model Sensitivity to Primary Inputs

Appendix A presents a detailed analysis of the sensitivity of α to changes in the parameters A, B, and C, and the primary inputs. In brief, α is at most linearly sensitive to changes in each of the primary inputs. This means that doubling a given input will at most cause either a doubling or halving of the α value. This will be seen in the sample results presented in Section 5.0.

4.0 Reasonable Ranges for Primary Input Values

To use the flowchart given in Figure 3, the user must first assign reasonable initial values to all primary model inputs. However, only the distance from the foundation to the source (L_T) below is easily determined from typical site assessment data, and the rest need to be estimated or inferred from available data, experience, intuition, and empirical correlations. The discussion below focuses on the rationale and basis for the ranges of primary model input values appearing in Table 2.

4.2 Reasonable Ranges of Values for the Primary Inputs

Table 2 summarizes reasonable ranges for the redefined set of primary inputs. The table is organized so that the primary inputs are divided into four groups:

- primary inputs reasonably estimated from available site assessment data: $\{L_T\}$
- primary inputs reasonably estimated from experience and intuition: $\{(V_B/A_B), \eta, L_{\text{crack}}, E_B\}$
- primary inputs reasonably estimated indirectly from literature data: $\{(Q_{\text{soil}}/Q_B)\}$
- primary inputs reasonably estimated from correlations and secondary inputs: $\{D_T^{\text{eff}} \text{ and } D_{\text{crack}}^{\text{eff}}\}$

It should be noted that each reasonable range of values was selected by professional judgement based on consideration of the literature, physical constraints, and experience. In this work, a reasonable range is one that spans the range of values representative of most sites (in the author's judgement); the reasonable range does not include extreme or unlikely values (e.g.,

depth to water of 2000 m). This approach, rather than a statistical data reduction, was used because the available data is limited and comes from a variety of unrelated studies (e.g., the E_B

Table 2. Summary of Recommendations for Reasonable Primary Input Values.

Primary Input	Definition	Reasonable Range	Comments	References
<i>parameters reasonably estimated from available site assessment data</i>				
L_T	Depth from foundation to the vapor source or other point of interest [m]	0.01 – 50 m	To be determined from site assessment data, sampling depths, or defined scenario	Experience
<i>parameters reasonably estimated from experience and intuition</i>				
(V_B/A_B)	Ratio of enclosed-space volume to exposed surface area [m]	2 – 3 m	Approximately equal to the height of the enclosed space (e.g., basement height or height of first-floor room for slab-on-grade construction)	Experience
L_{crack}	Foundation thickness [m]	0.15 – 0.5 m	Based on typical construction practices	Experience
η	Fraction of surface area with permeable cracks	0.0005 – 0.005	$\eta=0.01$ (worst-case) corresponds to finger-width cracks spaced 1-m apart and running across the floor; $\eta=0.0003$ corresponds roughly to a 0.1 cm floor-wall seam perimeter crack around a 225 m ² area	Intuition And (1)
E_B	Indoor air exchange rate [d ⁻¹]	4.8 – 24	Based on building ventilation/energy efficiency studies	(2) – (3)
<i>parameters reasonably estimated indirectly from literature data</i>				
Q_{soil}/Q_B	Ratio of the soil gas intrusion rate to the building ventilation rate	0.05 – 0.0001	Based on vapor attenuation coefficients reported for radon studies and contaminant vapor intrusion case studies	(4) – (8)
<i>parameters reasonably estimated from correlations and secondary inputs</i>				
D_T^{eff}	Effective overall vapor-phase diffusion coefficient between $z=L_T$ and the foundation	See Figure 4	Necessary to use empirical correlations and secondary inputs - Equations (2) and (3)	(9) – (11)
$D_{\text{crack}}^{\text{eff}}$	Effective overall vapor-phase diffusion coefficient through foundation cracks	See Figure 4	Necessary to use empirical correlations and secondary inputs - Equations (2) and (3)	(9) – (11)

(1) - Eaton and Scott (1984); (2) - ASHRAE (1985); (3) Kootz and Rector (1995); (4) - Mose and Mushrush (1999); (5) - Fischer et. al. (1996); (6) - Little et. al. (1992); (7) - Olson and Corsi (2001); (8) - Fitzpatrick and Fitzgerald (1996); (9) - Brooks and Corey (1966); (10) - Carsel and Parish (1988); (11) Johnson and Ettinger (1991); (12) - USEPA (1996).

range comes from a data set on one group of buildings, while (Q_{soil}/Q_B) ratios are derived from other studies with other buildings). Reasonable ranges are given here to provide a starting point for input selection, recognizing that appropriate site-specific inputs may fall outside these ranges for a few sites.

4.2.1 Primary Inputs Reasonably Estimated from Available Site Assessment Data $\{L_T\}$

If the Johnson and Ettinger (1991) model is being used to assess impacts at a specific site, then L_T is the distance (depth) below a foundation where the soil gas concentration is measured or inferred from another measurement (i.e., dissolved groundwater concentrations). Most values will range between 0.01 and 50 m, with many being concentrated in the 1 to 20 m range. If the model is being used to establish broadly applicable regulatory target levels, it is suggested that users apply the model for a range of L_T values (e.g., 0.1 and 10 m).

4.2.2 Primary Inputs Reasonably Estimated from Experience and Intuition:

$$\{(V_B/A_B), \eta, L_{\text{crack}}, E_B\}$$

Three of these inputs $\{(V_B/A_B), \eta, L_{\text{crack}}\}$ are assigned based on physical intuition, while E_B is based on experience recorded in the literature. The inputs $\{(V_B/A_B), \eta, L_{\text{crack}}\}$ characterize the construction of the enclosed space, which could be a basement or the first-floor of a slab-on-grade construction. (V_B/A_B) is the ratio of the enclosed-space volume to the exposed surface area; when A_B is approximately equal to the enclosed-space footprint then this ratio is equal to the height of the enclosed space. Thus, 2 to 3 m is a reasonable range of values for (V_B/A_B) , and most values will be concentrated in the 2.4 to 2.7 m range. A reasonable range for the foundation thickness (L_T) is 0.15 to 0.5 m, with most values being closer to 0.2 m.

The parameter η represents the ratio of the area of cracks to the total exposed area (A_B). The literature and our experience are of limited use in assigning this value, so we must resort to intuition. Here we imagine a worst-case scenario to be one where parallel 1-cm wide cracks traversing the foundation are spaced every 0.99-m. This scenario corresponds to $\eta=0.01$. We can also imagine a scenario where the foundation is relatively crack-free, but vapors can pass through the wall-floor seam. If the wall-floor seam crack is 0.1 cm wide (Eaton and Scott, 1984), then $\eta=0.0008$ for a 25 m² (250 ft²) footprint, $\eta=0.0004$ for a 100 m² (1000 ft²) footprint,

and $\eta=0.0003$ for a 225 m^2 (2400 ft^2) footprint. Given these scenarios, it seems unlikely that η will be much greater than 0.005 or much less than 0.0005.

Indoor air exchange rates for homes (E_B) have been reported by ASHRAE (1985), Koontz and Rector (1995) and Murray and Burmaster (1995). The Koontz and Rector (1995) and Murray and Burmaster (1995) results suggests that E_B values will typically fall in the 4.8 to 29 air exchanges per day range (0.2 to 1.2 air exchanges per hour), with most values being clustered around the mean of 14 air exchanges per day (0.6 air exchanges per hour). For commercial buildings, the minimum fresh air exchange rate is sometimes quantified in the building code. Note, the air exchange rates represents the amount of air exchanged with outdoor air, not the amount of air passed through a heating/air conditioning unit.

4.2.3 Primary Inputs Reasonably Estimated Indirectly from Literature Data: $\{(Q_{\text{soil}}/Q_B)\}$

As discussed above, (Q_{soil}/Q_B) is equal to the attenuation factor between soil gas directly below the foundation and indoor air (please note that it is equal to α only for that specific case; i.e., when $L_T \rightarrow 0$). Therefore, a search of the radon and contaminant transport literature was conducted to identify studies where both sub-slab and indoor air concentrations were reported. This data was then used to calculate $(Q_{\text{soil}}/Q_B)=(C_{\text{indoor}}/C_{\text{sub-slab}})$. Results show (Q_{soil}/Q_B) values of 0.0003 – 0.001 (Fischer et al., 1996), 0.003 – 0.02 (Mose and Mushrush, 1999), 0.0016 (Little et al., 1992), and 0.00006 – 0.0002 (Olson and Corsi, 2001). Fitzpatrick and Fitzgerald (1996) report values as high as 0.1. Of the studies listed above, all except the studies of Mose and Mushrush (1999) and Fitzpatrick and Fitzgerald (1996), involved focused studies of single buildings. Arguably the overall data set is limited, but it is supportive of a proposed reasonable range for (Q_{soil}/Q_B) between 0.0001 and 0.01.

4.2.4 Primary Inputs Reasonably Estimated from Correlations and Secondary Inputs: $\{D_T^{\text{eff}}$ and $D_{\text{crack}}^{\text{eff}}\}$

The primary inputs D_T^{eff} and $D_{\text{crack}}^{\text{eff}}$ can be measured (Johnson et al. 1998), but they are most often calculated using Equation (2) and the secondary inputs D^{air} , $D^{\text{H}_2\text{O}}$, H_i , θ_v , θ_m , and θ_T . Therefore, the discussion here focuses both on reasonable ranges of values for D^{air} , $D^{\text{H}_2\text{O}}$, H_i , θ_v , θ_m , and θ_T , as well as expectations for reasonable ranges of D_T^{eff} and $D_{\text{crack}}^{\text{eff}}$. Of these, the first three values are chemical-specific properties and the remaining are soil properties. The three soil properties are not independent because we can write:

$$\theta_v = \theta_T - \theta_m \quad (7)$$

If Equation (7) is substituted into Equation (2) and rearranged, then:

$$D^{\text{eff}} = D^{\text{air}} \theta_T^{1.33} [1 - S_m]^{3.33} \left\{ 1 + \left(\frac{D^{\text{H}_2\text{O}}}{H_i D^{\text{air}}} \right) \left(\frac{S_m}{1 - S_m} \right)^{3.33} \right\} \quad (8)$$

where $S_m = (\theta_m/\theta_T)$ is the moisture saturation. Equation (8) is written in such a way that the secondary inputs are $\{D^{\text{air}}, \theta_T, S_m, \text{ and } (D^{\text{H}_2\text{O}}/H_i D^{\text{air}})\}$. This form has been selected for two main reasons – it prevents users from selecting non-physical, or unreasonable combinations of θ_T , θ_m , and θ_v , and also because the second term within the $\{\}$ on the right-hand side is typically small for transport through the vadose zone.

The properties D^{air} , $D^{\text{H}_2\text{O}}$, and H_i are chemical-specific and are tabulated for many chemicals in the USEPA spreadsheets. For many chemicals D^{air} values range from about 0.1 – 1.0 m^2/d , $D^{\text{H}_2\text{O}}/D^{\text{air}}$ is usually about 10^{-4} , and H_i values for many aromatics and chlorinated solvents fall in the range 0.01 – 1 ($(\text{ug}/\text{m}^3\text{-air})/(\text{ug}/\text{m}^3\text{-H}_2\text{O})$). While diffusion coefficients typically fall within an order-of-magnitude range as indicated above, it is important to note that Henry's Law Constants range over several orders of magnitude and the range given above is only appropriate for the aromatic and chlorinated solvents considered (e.g., benzene, TCE, etc.).

Figure 4 presents the dependence of $(D^{\text{eff}}/D^{\text{air}})$ on θ_T , S_m , and H_i . In all plots, $D^{\text{H}_2\text{O}}/D^{\text{air}}=10^{-4}$. In Figure 4a, curves of $(D^{\text{eff}}/D^{\text{air}})$ vs. S_m are presented for $H_i=0.1$ ($(\text{ug}/\text{m}^3\text{-air})/(\text{ug}/\text{m}^3\text{-H}_2\text{O})$) and a range of θ_T . In Figure 4b, curves of $(D^{\text{eff}}/D^{\text{air}})$ vs. S_m are presented for $\theta_T=0.3$ and a range of H_i . For reference, typical residual moisture saturations for unconsolidated materials are generally: a) 0.05 – 0.10 for coarse-grained materials like sands and gravels, b) 0.10 - 0.30 for finer-grained mixtures of sands, silts and clays, and c) as high as 0.50 for clayey materials having low proportions of sands and silts (e.g., Carsel and Parrish 1988). Reasonable total porosity values for unconsolidated materials range from about 0.3 [$\text{m}^3\text{-pores}/\text{m}^3\text{-soil}$] for well-graded/poorly sorted sand, gravel and silt mixtures to about 0.50 [$\text{m}^3\text{-pores}/\text{m}^3\text{-soil}$] for clays. For a given soil type, the reasonable range of θ_T and S_m values is relatively narrow (roughly 10% above and below an average value for total porosity and roughly 50% above and below an average value for S_m). It is important to note that these generalizations are specific to well-drained vadose zone materials at residual saturations. Perched water zones, or near-surface soils in high recharge areas may have greater moisture saturations, for example $S_m>0.90$ for a

perched water zone. In Figure 4a and 4b, the regions of S_m values corresponding to typical drained vadose zone soil types and perched/saturated zone conditions are indicated.

Figure 4a allows examination of the dependencies of D^{eff} on total porosity θ_T and moisture saturation S_m . At any S_m value, D^{eff} increases by a factor of about 2.5 across the full range of θ_T values displayed (0.25 to $0.50 \text{ m}^3\text{-pores/m}^3\text{-soil}$). In the reasonable range of typical drained conditions, increases in S_m of $0.1 \text{ m}^3\text{-water/m}^3\text{-pores}$ for any given θ_T correspond to 50% decreases in D^{eff} . Thus, if one considers the reasonable range of uncertainty in S_m and θ_T values for a given qualitative soil description (i.e., sands and gravels, mixed sands/silts/clays, or clays), the uncertainty in D^{eff} values is roughly 50% about the average value for the reasonable range of conditions for that soil descriptor. In the range of reasonable saturated/perched conditions, changes in S_m have little discernible effect on D^{eff} .

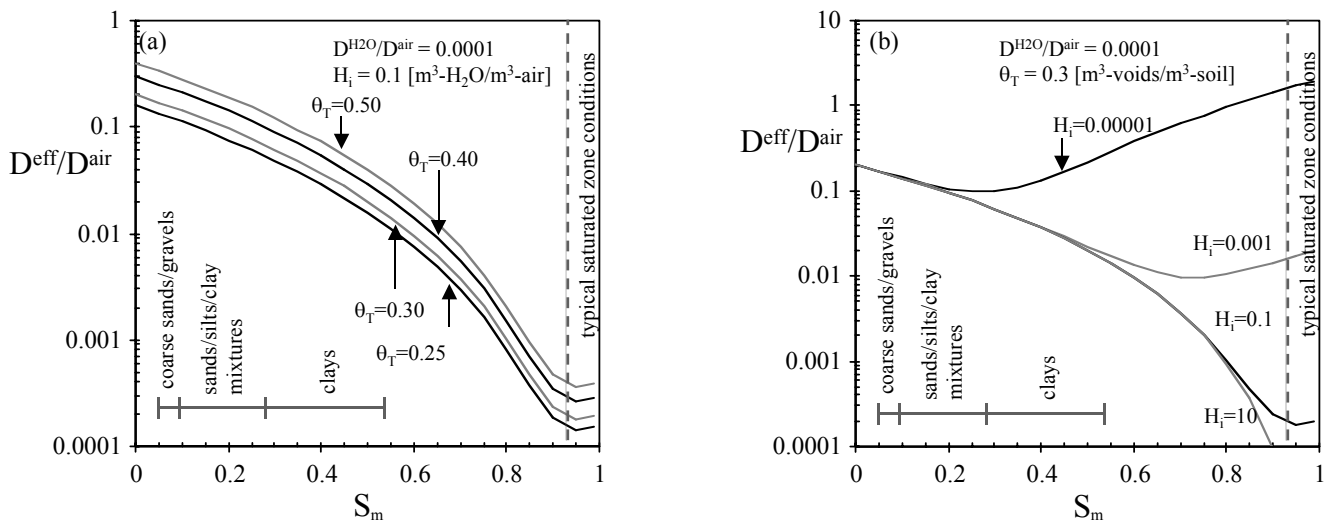


Figure 4. Dependence of $D^{\text{eff}}/D^{\text{air}}$ on moisture saturation $S_m = (\theta_m/\theta_T)$ for: a) $H_i = 0.1$ ($(\text{ug/m}^3\text{-air})/(\text{ug/m}^3\text{-H}_2\text{O})$) and a range of θ_T , and b) $\theta_T = 0.30$ and a range of H_i values.

Figure 4b allows examination of the dependencies of D^{eff} on Henry's Law Constant H_i and moisture saturation S_m . As can be seen, for all $H_i > 0.00001$ ($(\text{ug/m}^3\text{-air})/(\text{ug/m}^3\text{-H}_2\text{O})$), changes in H_i have little effect on D^{eff} when $S_m < 0.30$ ($\text{m}^3\text{-pores/m}^3\text{-soil}$). This dependence occurs because the vapor-phase diffusive flux contribution is significantly greater than the moisture-phase dissolved flux under these conditions (i.e.; the first term on the right-hand-side of

equation (2) is dominant). Changes in H_i have linear effects on D^{eff} in the region typical of saturated conditions (e.g., D^{eff} increases by 10 times when H_i is decreased by a factor of 10).

Based on the results given in Figures 4a and 4b, and consideration of Equation (8), the following generalizations can be stated: a) unless $H_i < 10^{-6}$ ((ug/m³-air)/(ug/m³-H₂O)), reasonable D^{eff} ranges for drained vadose zone materials are: a) $0.1D^{\text{air}}$ to $0.2D^{\text{air}}$ for coarse sands and gravels, and b) $0.06D^{\text{air}}$ to $0.2D^{\text{air}}$ for sand/silt/clay mixtures. For clays at residual saturations in the vadose zone, the reasonable D^{eff} range is $0.02D^{\text{air}}$ to $0.04D^{\text{air}}$, provided that $H_i > 0.001$ ((ug/m³-air)/(ug/m³-H₂O)).

For saturated materials, a reasonable D^{eff} range is $0.2D^{\text{H}_2\text{O}}/H_i$ to $0.4 D^{\text{H}_2\text{O}}/H_i$, and these values may be much less than, comparable to, or even greater than the D^{eff} values for vadose conditions as shown in Figure 4b.

Some readers may feel that the discussion above is contrary to conventional wisdom, as many practitioners believe D^{eff} to be very sensitive to subtle moisture content changes and that D^{eff} for saturated conditions is always less than D^{eff} for vadose zone conditions. As can be seen in Figure 4, D^{eff} does change significantly across the full range of moisture saturations; however, D^{eff} does not change significantly when constrained to a reasonable range for a given soil descriptor. For example, it would be incorrect to assign a value of $S_m=0.50$ to coarse sands and gravels in the vadose zone. Also, D^{eff} for near-saturated conditions can be greater than D^{eff} for unsaturated conditions when $H_i > 0.00001$ ((ug/m³-air)/(ug/m³-H₂O)).

5.0 Sample Use of the Figure 3 Flowchart with Reasonable Values of Inputs

Table 3 presents primary and secondary inputs for four hypothetical scenarios; two scenarios (1 and 2) represent shallow soil gas and shallow dissolved groundwater source settings and the others (3 and 4) are examples of deep soil gas and deep dissolved groundwater source settings. The parameters A, B, and C are presented for each scenario along with the critical and non-critical primary inputs indicated by the Figure 3 flowchart.

In reviewing the parameters, it can be seen that $A \ll 1$, $B > 3$, and $C < 0.01$ for all four cases. The Figure 3 flowchart indicates that these are settings in which advection is the dominant mechanism of transport across the foundation ($B > 3$). It also indicates that the primary inputs $\{D_{\text{crack}}^{\text{eff}}, L_{\text{crack}}, \text{ and } \eta\}$ are non-critical for the four example settings. To examine if this

conclusion generally holds true, minimum and maximum B values can be calculated for the input ranges given in Table 2. Those B values range roughly from 0.4 to 7×10^4 , and this suggests that advection is the dominant mechanism for transport across the foundation for most settings, and that the primary inputs $\{D_{\text{crack}}^{\text{eff}}, L_{\text{crack}}, \text{ and } \eta\}$ are non-critical for most settings. This conclusion is consistent with the radon intrusion literature, where advection is believed to be the dominant mechanism for transporting radon across the foundation (Nazaroff 1992).

The four example scenarios represent two of the flowchart's $B > 3$ branches; Scenarios 1 and 3 correspond to $0.1 < (A/C) < 10$, and Scenarios 2 and 4 correspond to $(A/C) < 0.1$. Both branches indicate that (V_B/A_B) , L_T , D_T^{eff} , and E_B could be critical parameters, while the $0.1 < (A/C) < 10$ branch also includes (Q_{soil}/Q_B) as a critical input. Again, as discussed previously, variations with changes in these inputs are expected to be at most linear, and this will be tested below.

Tables 4a through 4d present results from conventional sensitivity analyses for these four scenarios. The purpose of this exercise is to provide verification that the Figure 3 flowchart provides reasonable results, and also to give the reader an opportunity to see how α varies with sequential changes in inputs. In each case, the effect of sequential 50% increases in input values is examined through changes in vapor attenuation coefficients α . In addition, a normalized measure of sensitivity is presented for each of the inputs. This measure of sensitivity is the ratio of the magnitude of the percentage change in α divided by the magnitude of the percentage change in the input value. For reference, a value of zero indicates that α does not vary with changes in a particular input, and those inputs would be considered to be non-critical. Values close to unity indicate near-linear response within changes in that input. As can be seen, the flowchart identifies the non-critical and critical parameters suggested by the conventional sensitivity analysis.

In the cases of Scenarios 2 and 4, the conventional analysis results suggest that α is not sensitive to changes in L_T , whereas the flowchart does not indicate this to be a non-critical parameter. Scenarios 2 and 4 correspond to cases where the capillary fringe is the dominant diffusion resistance, and in those cases D_T^{eff} and L_T can not be varied independently (see Equation (3)). Under these conditions, D_T^{eff} varies with L_T in such a way that the ratio D_T^{eff}/L_T changes little as L_T changes. Consequently α changes little with variation in L_T as α depends on the ratio D_T^{eff}/L_T .

In reviewing the sensitivity of model results to changes in inputs for the four cases, it can be seen that changes in output with changes in input is often approximately linear (e.g., the sensitivity measure is approximately unity), and that the sensitivity is low to changes in most parameter values. Again, this illustrates that, contrary to some practitioners beliefs, the Johnson and Ettinger (1991) model output is generally affected by only a small number of inputs, provided that inputs are varied across reasonable ranges of values.

The results also show that use of the flowchart-based approach leads to reliable identification of non-critical inputs and potentially critical inputs. Generally, the results in Tables 4a through 4d suggest that the non-critical inputs identified by Figure 3 are indeed non-critical, and that the actual number of critical inputs may be less than that suggested by Figure 3.

6.0 Summary

It is difficult for users to develop a thorough understanding of the relationships between model inputs and outputs so that they can identify critical inputs when applying the Johnson and Ettinger (1991) model or when using the USEPA spreadsheet implementation of this model. The parametric analysis conducted above shows that model output is controlled by three dimensionless parameters, and that if one understands how output varies with changes in these parameters, then the dependence on individual inputs can also be correctly deduced. The results also show that the sets of critical and non-critical inputs are not fixed, but that they are dictated by the specific combination of the three parameters. Thus, a spreadsheet approach can help users identify the critical and non-critical inputs for each application. Reasonable ranges for the primary inputs are also tabulated here to provide users a basis for comparison with their input sets. Sample use of the flowchart for four scenarios suggests that some inputs are non-critical for most applications. Use of the four scenarios also shows that the simplified flowchart approach leads to the same conclusions as a more lengthy and complex conventional sensitivity analysis.

Table 3. Primary and Secondary Inputs for Four Scenarios.

Primary Input	Secondary Input	Units	Scenario 1 Shallow Soil Gas Source	Scenario 2 Shallow Ground Water Source	Scenario 3 Deep Soil Gas Source	Scenario 4 Deep Ground Water Source
V_B/A_B	-	[m]	2.4	2.4	2.4	2.4
L_{crack}	-	[m]	0.15	0.15	0.15	0.15
η	-	[m ² -cracks/m ² -total]	0.001	0.001	0.0005	0.0005
Q_{soil}/Q_B	-	[dim]	0.01	0.01	0.001	0.001
E_B	-	[d ⁻¹]	14	14	20	20
L_T	-	[m]	0.2	0.2	10	10
D_{crack}^{eff}	θ_T	[m ³ -voids/m ³ -soil]	0.3	0.3	0.3	0.3
	S_m	[dim]	0.1	0.1	0.1	0.1
	H_i	[m ³ -H ₂ O/m ³ -air]	0.1	0.1	0.1	0.1
	D^{air}	[m ² /d]	1.0	1.0	1.0	1.0
	D^{H_2O}	[m ² /d]	10 ⁻⁴	10 ⁻⁴	10 ⁻⁴	10 ⁻⁴
			[m ² /d]	0.14	0.14	0.14
D_T^{eff}	θ_T - vadose	[m ³ -voids/m ³ -soil]	0.3	0.3	0.35	0.35
	S_m - vadose	[dim]	0.1	0.1	0.2	0.2
	θ_T - cap	[m ³ -voids/m ³ -soil]	NA	0.3	NA	0.4
	S_m - cap	[dim]	NA	0.90	NA	0.90
	L_{cap}	[m]	NA	0.10	NA	0.30
	H_i	[m ³ -H ₂ O/m ³ -air]	0.1	0.1	0.1	0.1
	D^{air}	[m ² /d]	1.0	1.0	1.0	1.0
	D^{H_2O}	[m ² /d]	10 ⁻⁴	10 ⁻⁴	10 ⁻⁴	10 ⁻⁴
		[m ² /d]	0.14	0.00036	0.14	0.012
		Parameter A	0.02	0.00007	0.00025	0.000019
		Parameter B	360	360	100	100
		Parameter C	0.01	0.01	0.001	0.001
		Critical Primary Inputs from Flowchart	$V_B/A_B, L_T,$ $D_{crack}^{eff}, E_B,$ Q_{soil}/Q_B	$V_B/A_B, L_T,$ D_{crack}^{eff}, E_B	$V_B/A_B, L_T,$ $D_{crack}^{eff}, E_B,$ Q_{soil}/Q_B	$V_B/A_B, L_T,$ D_{crack}^{eff}, E_B
		Non-Critical Primary Inputs from Flowchart	$L_{crack},$ D_{crack}^{eff}, η	$L_{crack},$ $D_{crack}^{eff}, \eta,$ Q_{soil}/Q_B	$L_{crack},$ D_{crack}^{eff}, η	$L_{crack},$ $D_{crack}^{eff}, \eta,$ Q_{soil}/Q_B
		α	6.8×10^{-3}	6.9×10^{-5}	2.0×10^{-4}	1.8×10^{-5}

Cap = capillary fringe

Table 4a. Sensitivity Analysis for Scenario 1 – Shallow Soil Gas Source – Showing the Effects of Sequential Input Variation.

Primary Input	Secondary Input	Units	Scenario 1 Shallow Soil Gas Source Initial Inputs	Scenario 1 Shallow Soil Gas Source Changed Inputs (1.5X)	Result: New α Estimate	Sensitivity [%-alpha change/%-input change)
Initial Input Set					6.8×10^{-3}	
Sequential Changes						
V_B/A_B	-	[m]	2.4	3.6	5.9×10^{-3}	0.29
L_{crack}	-	[m]	0.15	0.23	5.9×10^{-3}	0
η	-	[m ² -cracks/m ² -total]	0.001	0.0015	5.9×10^{-3}	0
Q_{soil}/Q_B	-	[dim]	0.01	0.015	7.3×10^{-3}	0.48
E_B	-	[d ⁻¹]	14	21	5.8×10^{-3}	0.41
L_T	-	[m]	0.2	0.3	4.4×10^{-3}	0.47
D_{crack}^{eff}	θ_T	[m ³ -voids/m ³ -soil]	0.3	0.45	4.4×10^{-3}	0
	S_m	[dim]	0.1	0.15	4.4×10^{-3}	0
	H_i	[m ³ -H ₂ O/m ³ -air]	0.1	No change	4.4×10^{-3}	NA
	D^{air}	[m ² /d]	1.0	No change	4.4×10^{-3}	NA
	D^{H_2O}	[m ² /d]	10^{-4}	No change	4.4×10^{-3}	NA
			[m ² /d]	Calculated	Calculated	
D_T^{eff}	θ_T - vadose	[m ³ -voids/m ³ -soil]	0.3	0.45	6.3×10^{-3}	0.83
	S_m - vadose	[dim]	0.1	0.15	5.9×10^{-3}	0.22
	θ_T - cap	[m ³ -voids/m ³ -soil]	NA	No change	5.9×10^{-3}	NA
	S_m - cap	[dim]	NA	No change	5.9×10^{-3}	NA
	L_{cap}	[m]	NA	No change	5.9×10^{-3}	NA
	H_i	[m ³ -H ₂ O/m ³ -air]	0.1	No change	5.9×10^{-3}	NA
	D^{air}	[m ² /d]	1.0	No change	5.9×10^{-3}	NA
	D^{H_2O}	[m ² /d]	10^{-4}	No change	5.9×10^{-3}	NA
		[m ² /d]	Calculated	Calculated		

Cap = capillary fringe

Results Suggested by Flowchart:

- Critical Parameters – $\{V_B/A_B, L_T, D_T^{eff}, E_B, Q_{soil}/Q_B\}$
- Non-Critical Parameters – $\{L_{crack}, D_{crack}^{eff}, \eta\}$

Table 4b. Sensitivity Analysis for Scenario 2 – Shallow Groundwater Source – Showing the Effects of Sequential Input Variation.

Primary Input	Secondary Input	Units	Scenario 2 Shallow Ground Water Source Initial Inputs	Scenario 2 Shallow Ground Water Source Changed Inputs (1.5X)	Result: New α Estimate	Sensitivity [%-alpha change/%-input change)
Initial Input Set					6.9×10^{-5}	
Sequential Changes						
V_B/A_B	-	[m]	2.4	3.6	4.7×10^{-5}	0.64
L_{crack}	-	[m]	0.15	0.23	4.7×10^{-5}	0
η	-	[m ² -cracks/m ² -total]	0.001	0.0015	4.7×10^{-5}	0
Q_{soil}/Q_B	-	[dim]	0.01	0.015	4.7×10^{-5}	0
E_B	-	[d ⁻¹]	14	21	3.1×10^{-5}	0.68
L_T	-	[m]	0.2	0.3	3.1×10^{-5}	0
D_{crack}^{eff}	θ_T	[m ³ -voids/m ³ -soil]	0.3	0.45	3.1×10^{-5}	0
	S_m	[dim]	0.1	0.15	3.1×10^{-5}	0
	H_i	[m ³ -H ₂ O/m ³ -air]	0.1	No change	3.1×10^{-5}	NA
	D^{air}	[m ² /d]	1.0	No change	3.1×10^{-5}	NA
	D^{H_2O}	[m ² /d]	10^{-4}	No change	3.1×10^{-5}	NA
			[m ² /d]	Calculated	Calculated	
D_T^{eff}	θ_T - vadose	[m ³ -voids/m ³ -soil]	0.3	0.45	3.1×10^{-5}	0
	S_m - vadose	[dim]	0.1	0.15	3.1×10^{-5}	0
	θ_T - cap	[m ³ -voids/m ³ -soil]	0.3	0.45	5.3×10^{-5}	1.4
	S_m - cap	[dim]	0.90	0.99	4.4×10^{-5}	1.7
	L_{cap}	[m]	0.1	0.15	2.9×10^{-5}	0.66
	H_i	[m ³ -H ₂ O/m ³ -air]	0.1	No change	2.9×10^{-5}	NA
	D^{air}	[m ² /d]	1.0	No change	2.9×10^{-5}	NA
	D^{H_2O}	[m ² /d]	10^{-4}	No change	2.9×10^{-5}	NA
		[m ² /d]	Calculated	Calculated		

Cap = capillary fringe

Results Suggested by Flowchart:

- Critical Parameters – $\{V_B/A_B, L_T, D_T^{eff}, E_B\}$
- Non-Critical Parameters – $\{L_{crack}, D_{crack}^{eff}, \eta, Q_{soil}/Q_B\}$

Table 4c. Sensitivity Analysis for Scenario 3 – Deep Soil Gas Source – Showing the Effects of Sequential Input Variation.

Primary Input	Secondary Input	Units	Scenario 3 Deep Soil Gas Source Initial Inputs	Scenario 3 Deep Soil Gas Source Changed Inputs (1.5X)	Result: New α Estimate	Sensitivity [%-alpha change/%-input change)
Initial Input Set					2.0×10^{-4}	
Sequential Changes						
V_B/A_B	-	[m]	2.4	3.6	1.4×10^{-4}	0.60
L_{crack}	-	[m]	0.15	0.23	1.4×10^{-4}	0
η	-	[m ² -cracks/m ² -total]	0.0005	0.00075	1.4×10^{-4}	0
Q_{soil}/Q_B	-	[dim]	0.001	0.0015	1.5×10^{-4}	0.14
E_B	-	[d ⁻¹]	20	30	1.0×10^{-4}	0.67
L_T	-	[m]	10	15	6.9×10^{-5}	0.62
D_{crack}^{eff}	θ_T	[m ³ -voids/m ³ -soil]	0.3	0.45	6.9×10^{-5}	0
	S_m	[dim]	0.1	0.15	6.9×10^{-5}	0
	H_i	[m ³ -H ₂ O/m ³ -air]	0.1	No change	6.9×10^{-5}	NA
	D^{air}	[m ² /d]	1.0	No change	6.9×10^{-5}	NA
	D^{H_2O}	[m ² /d]	10^{-4}	No change	6.9×10^{-5}	NA
			[m ² /d]	Calculated	Calculated	
D_T^{eff}	θ_T - vadose	[m ³ -voids/m ³ -soil]	0.35	0.53	1.2×10^{-4}	1.5
	S_m - vadose	[dim]	0.2	0.3	7.7×10^{-5}	0.72
	θ_T - cap	[m ³ -voids/m ³ -soil]	NA	NA	7.7×10^{-5}	NA
	S_m - cap	[dim]	NA	NA	7.7×10^{-5}	NA
	L_{cap}	[m]	NA	NA	7.7×10^{-5}	NA
	H_i	[m ³ -H ₂ O/m ³ -air]	0.1	No change	7.7×10^{-5}	NA
	D^{air}	[m ² /d]	1.0	No change	7.7×10^{-5}	NA
	D^{H_2O}	[m ² /d]	10^{-4}	No change	7.7×10^{-5}	NA
		[m ² /d]	Calculated	Calculated		

Cap = capillary fringe

Results Suggested by Flowchart:

- Critical Parameters – { V_B/A_B , L_T , D_T^{eff} , E_B , Q_{soil}/Q_B }
- Non-Critical Parameters – { L_{crack} , D_{crack}^{eff} , η }

Table 4d. Sensitivity Analysis for Scenario 4 – Deep Groundwater Source – Showing the Effects of Sequential Input Variation.

Primary Input	Secondary Input	Units	Scenario 4 Deep Ground Water Source Initial Inputs	Scenario 4 Deep Ground Water Source Changed Inputs (1.5X)	Result: New α Estimate	Sensitivity [%-alpha change/%-input change)
Initial Input Set					1.8×10^{-5}	
Sequential Changes						
V_B/A_B	-	[m]	2.4	3.6	1.2×10^{-5}	0.67
L_{crack}	-	[m]	0.15	0.23	1.2×10^{-5}	0
η	-	[m ² -cracks/m ² -total]	0.0005	0.00075	1.2×10^{-5}	0
Q_{soil}/Q_B	-	[dim]	0.001	0.0015	1.2×10^{-5}	0
E_B	-	[d ⁻¹]	20	30	8.3×10^{-6}	0.62
L_T	-	[m]	10	15	8.0×10^{-6}	0.075
D_{crack}^{eff}	θ_T	[m ³ -voids/m ³ -soil]	0.3	0.45	8.0×10^{-6}	0
	S_m	[dim]	0.1	0.15	8.0×10^{-6}	0
	H_i	[m ³ -H ₂ O/m ³ -air]	0.1	No change	8.0×10^{-6}	NA
	D^{air}	[m ² /d]	1.0	No change	8.0×10^{-6}	NA
	D^{H_2O}	[m ² /d]	10^{-4}	No change	8.0×10^{-6}	NA
			[m ² /d]	Calculated	Calculated	
D_T^{eff}	θ_T - vadose	[m ³ -voids/m ³ -soil]	0.35	0.53	8.3×10^{-6}	0.075
	S_m - vadose	[dim]	0.2	0.3	8.0×10^{-6}	0.075
	θ_T - cap	[m ³ -voids/m ³ -soil]	0.35	0.53	1.3×10^{-5}	1.25
	S_m - cap	[dim]	0.90	0.99	1.1×10^{-5}	0.31
	L_{cap}	[m]	0.3	0.45	7.7×10^{-6}	0.6
	H_i	[m ³ -H ₂ O/m ³ -air]	0.1	No change	7.7×10^{-6}	NA
	D^{air}	[m ² /d]	1.0	No change	7.7×10^{-6}	NA
	D^{H_2O}	[m ² /d]	10^{-4}	No change	7.7×10^{-6}	NA
		[m ² /d]	Calculated	Calculated		

Cap = capillary fringe

Results Suggested by Flowchart:

- Critical Parameters – $\{V_B/A_B, L_T, D_T^{eff}, E_B\}$
- Non-Critical Parameters – $\{L_{crack}, D_{crack}^{eff}, \eta, Q_{soil}/Q_B\}$

References

- American Society of Heating Refrigerating and Air Conditioning Engineers (ASHRAE). 1985. ASHRAE Handbook (1985) Fundamentals. Chapter 22. Atlanta, GA.
- Brooks, R.H. and Corey. 1966. Properties of Porous Media Affecting Fluid Flow. ASCE J. Irrig. Drainage Div.. 72(IR2), 61-88.
- Carsel, R.F. and R.S. Parrish. 1988. Developing Joint Probability Distributions of Soil Water Retention Characteristics. Water Resources Research. 24(5). 755-769.
- Eaton, R.S. and A.G. Scott. 1984. Understanding Radon Transport Into Houses. Radiation Protection Dosimetry. 7. 251-253.
- Fischer, M.L., A.J. Bentley, K.A. Dunkin, A.T. Hodgson, W.W. Nazaroff, R.G. Sextro, and J.M. Daisey. 1996. Factors Affecting Indoor Air Concentrations of Volatile Organic Compounds at a Site of Subsurface Gasoline Contamination. Environ. Sci. Technol.. 30 (10). 2948-2957
- Fitzpatrick, N.A. and J.J. Fitzgerald. 1996. An Evaluation of Vapor Intrusion Into Buildings Through a Study of Field Data. Presented at the 11th Annual Conference on Contaminated Soils. University of Massachusetts – Amherst. October.
- Hers, I., R. Zapfe-Gilje, L. Li, and J. Atwater. 2001. The Use of Indoor Air Measurements to Evaluate Intrusion of Subsurface VOC Vapors into Buildings. J. Air & Waste Manage. Assoc.. 51. 1318-1331.
- Hers, I., R. Zapf-Gilje, P. C. Johnson, and L. Li. 2002. Evaluation of the Johnson and Ettinger Model for Prediction of Indoor Air Quality. Accepted for publication in Ground Water Monitoring and Remediation.
- Johnson, P.C. and R.A. Ettinger. 1991. Heuristic Model for Predicting the Intrusion Rate of Contaminant Vapors Into Buildings. Environ. Sci. Technol.. 25. 1445-1452.
- Johnson, P.C., C. Bruce. R.L. Johnson, and M.W. Kemblowski. 1998. In Situ Measurement of Effective Vapor-Phase Porous Medium Diffusion Coefficients. Environmental Science and Technology. 32. 3405-3409.
- Johnson, P.C., R.L. Johnson, and M.W. Kemblowski. 1998. Assessing the Significance of Subsurface Contaminant Migration to Enclosed Spaces: Site-Specific Alternatives to Generic Estimates. American Petroleum Institute Publication No. 4674. December.

Johnson, P.C., R.L. Johnson, and M.W. Kemblowski. 1999. Assessing the Significance of Vapor Migration to Enclosed-Spaces on a Site-Specific Basis. *Journal of Soil Contamination*. 8 (3). 389 - 421.

Johnson, P.C., R.A. Ettinger, J. Kurtz, R. Bryan, and J.E. Kester. 2002a. Migration of Soil Gas Vapors to Indoor Air: Determining Vapor Attenuation Factors Using a Screening-Level Model and Field Data from the CDOT-MTL Denver, Colorado Site. *American Petroleum Institute Bulletin No.16*. April.

Johnson, P. C., V. A. Hermes, S. Roggemans. 2002b. An Oxygen-Limited Hydrocarbon Vapor Migration Attenuation Screening Model. In preparation.

Koontz, M.D. and H.E. Rector. 1995. Estimation of Distributions for Residential Air Exchange Rates. EPA Contract No. 68-D9-0166, Work Assignment No. 3-19. USEPA Office of Pollution Prevention and Toxics. Washington, D.C.

Little, J.C., J.M. Daisey, W.W. Nazaroff. 1992. Transport of Subsurface Contaminants into Buildings: An Exposure Pathway for Volatile Organics. *Environ. Sci. Technol.* 26. 2058-2066.

Millington, R. J., Gas Diffusion in Porous Media, *Science*, 1959, 130, 100-102.

Millington, R. J. and J. P. Quirk,. 1961. Permeability of Porous Solids, *Trans. Faraday Soc.* 57. 1200-1207.

Millington, R. J. and R. C. Shearer. 1971. Diffusion in Aggregated Porous Media, *Soil Sci.* 111. 372-378.

Murray, D.M. and D.E. Burmaster. 1995. Residential Air Exchange Rates in the United States: Empirical and Estimated Parametric Distributions by Season and Climactic Region. *Risk Analysis*. 15. 459-465.

Mose, D.G. and G.W. Mushrush. 1999. Comparisons Between Soil Radon and Indoor Radon. *Energy Sources*. 21. 723-731.

Nazaroff, W.W.. 1992. Radon Transport from Soil to Air. *Review of Geophysics*. 30 (2). 137 – 160.

Olson, D.A. and R.L. Corsi. 2001. Characterizing Exposure to Chemicals from Soil Vapor Intrusion Using a Two-Compartment Model. *Atmospheric Environment*. 35. 4201-4209.

Robinson, A.L., R.G. Sextro, W.J. Fisk. 1997. Soil-Gas Entry Into an Experimental Basement Driven by Atmospheric Pressure Fluctuations – Measurements, Spectral Analysis, and Model Comparison. *Atmospheric Environment*. 31 (10). 1477-1485.

Robinson, A.L. and R.G. Sextro. 1997. Radon Entry into Buildings Driven by Atmospheric Pressure Fluctuations. *Environ. Sci. Technol.*. 31 (6). 1742-1748.

USEPA. 1997. User's Guide for the Johnson and Ettinger (1991) Model for Subsurface Vapor Intrusion Into Buildings. Prepared by Environmental Quality Management, Inc.. Contract No. 68-D30035. September 1997.

[http://www.epa.gov/superfund/programs/risk/airmodel/johnson_ettinger.htm]

USEPA. 1997 - 2000. Spreadsheets for the Johnson and Ettinger (1991) Model. Prepared by Environmental Quality Management, Inc..

[http://www.epa.gov/superfund/programs/risk/airmodel/johnson_ettinger.htm]

USEPA. 2001. Draft Supplemental Guidance for Evaluating the Vapor Intrusion to Indoor Air Pathway. November.

Appendix A: Understanding Relationships Between Model Inputs and α -Values, and the Identification of Critical and Non-Critical Primary Inputs

There are eight primary Johnson and Ettinger (1991) model inputs; with the introduction of secondary inputs, a model application may involve 20 or more inputs. Therefore, it is unlikely that traditional methods (i.e., sequential variation of individual inputs and inspection of output) will be of use for developing an understanding of the relationships between individual inputs and model output.

A parametric analysis of the Johnson and Ettinger (1991) equation is conducted below. It will be shown that model output depends on only three basic parameters. These “parameters” are dimensionless groupings of the primary inputs. Furthermore it will be shown that these parameters have physical relevance and the dependence of α on individual primary and secondary inputs can easily be deduced if one understands the relationships between these parameters and α . The results of this parametric analysis were used to create the flowchart-based approach presented in Figure 3 of the main body of this report. That figure presents a generalized approach for identifying the critical and non-critical model inputs.

For the purposes of this discussion a “non-critical input” is one that can be varied without causing significant changes in the model output (e.g., less than a 20% variation in output across the likely range of values for that input). All other inputs are defined to be “critical inputs”. It is important to note, however, that use of the term “critical” in this context is not meant to imply that large changes in model output are caused by small changes in the model inputs. In fact, it will be seen that changes in α are at most linear with changes in primary input values.

A.1 Parametric Analysis of the Johnson and Ettinger (1991) Algorithm

While the Johnson and Ettinger (1991) algorithm is often written in terms of eight primary inputs, it can also be written much more simply in terms of three dimensionless parameters:

$$\alpha = \frac{[A] \exp(B)}{\exp(B) + [A] + \left[\frac{A}{C} \right] (\exp(B) - 1)} \quad (A1)$$

where:

$$A = \left[\frac{D_T^{\text{eff}} A_B}{Q_B L_T} \right], \quad B = \left[\frac{Q_{\text{soil}} L_{\text{crack}}}{D_{\text{crack}}^{\text{eff}} \eta A_B} \right], \quad C = \left[\frac{Q_{\text{soil}}}{Q_B} \right] \quad (\text{A2})$$

or:

$$A = \left[\frac{D_T^{\text{eff}}}{E_B \left(\frac{V_B}{A_B} \right) L_T} \right], \quad B = \left[\frac{\left(\frac{Q_{\text{soil}}}{Q_B} \right) E_B \left(\frac{V_B}{A_B} \right) L_{\text{crack}}}{D_{\text{crack}}^{\text{eff}} \eta} \right], \quad C = \left[\frac{Q_{\text{soil}}}{Q_B} \right] \quad (\text{A3})$$

and:

- A_B = the surface area of the enclosed space in contact with soil [m^2]
- α = $(C_{\text{indoor}}/C_{\text{source}})$; C_{indoor} denotes the indoor air concentration and C_{source} is the vapor concentration at some depth (both in consistent units)
- $D_{\text{crack}}^{\text{eff}}$ = the effective overall vapor-phase diffusion coefficient through the walls and foundation cracks [m^2/d]
- D_T^{eff} = the effective overall vapor-phase diffusion coefficient between the foundation and the depth L_T [m^2/d]
- L_{crack} = the enclosed space foundation thickness [m]
- L_T = the distance (depth) to the vapor source or other point of interest below foundation [m]
- Q_B = the enclosed space volumetric air flow rate [m^3/d]; usually estimated to be the product of the enclosed-space volume (V_B [m^3]) and the indoor air exchange rate (E_B [1/d])
- Q_{soil} = the pressure-driven soil gas flow rate from the subsurface into the enclosed space [m^3/d]
- η = the fraction of enclosed space surface area open for vapor intrusion [m^2/m^2]; this is sometimes referred to as the “crack factor” and is estimated to be the total area of cracks, seams, and any perforations of surfaces in contact with soil divided by the total area in contact with soil.

This parametric form of the Johnson and Ettinger (1991) algorithm provides a valuable tool for developing an understanding of the relationships between model inputs and α . If one

can understand the relationships between these three parameters and the model output, then the dependence on individual primary or secondary inputs can be deduced.

It is useful to note that each of the parameters has physical relevance:

- $A (=D_T^{\text{eff}} A_B/Q_B L_T)$ is equal to the vapor attenuation coefficient for cases where there is no foundation (e.g., a bare dirt floor) and diffusion through the soil to the foundation is the controlling mechanism.
- $B (=Q_{\text{soil}} L_{\text{crack}}/D_{\text{crack}}^{\text{eff}} A_B \eta)$ is a measure of the significance of the two mechanisms responsible for transporting chemical vapors across the building foundation (advection and diffusion). If $B \gg 1$ then advection is primarily responsible for chemical transport across the foundation; if $B \ll 1$, then diffusion is primarily responsible for chemical transport across the foundation.
- $C (=Q_{\text{soil}}/Q_B)$ is equal to the vapor attenuation coefficient between vapors immediately below the foundation and indoor air (e.g., $L_T \rightarrow 0$), provided that advection is the mechanism responsible for transport across the foundation (i.e., $B \gg 1$).

In addition, combinations of these parameters also have physical relevance:

- The combination $(AB/C) (=D_T^{\text{eff}} L_{\text{crack}}/L_T D_{\text{crack}}^{\text{eff}} \eta)$ is a measure of the significance of diffusive transport through the soil relative to diffusive transport through the foundation. As shown below, it appears in Equation A4 when $B \ll 1$. If $(AB/C) \gg 1$ then diffusion through the foundation is the overall rate-limiting process; if $(AB/C) \ll 1$ then diffusion through the soil is the overall rate-limiting process.
- The combination $(B/C) (=Q_B L_{\text{crack}}/A_B D_{\text{crack}}^{\text{eff}} \eta)$ is equal to the vapor attenuation coefficient between vapors immediately below the foundation and indoor air (e.g., $L_T \rightarrow 0$), provided that diffusion through the foundation is the mechanism responsible for transport across the foundation (i.e., $B \ll 1$). It appears in Equation A4 when $B \ll 1$ and $(AB/C) > 10(1+A)$.

Figure A1 presents a series of four graphs that illustrate the dependence of α on the three parameters A, B, and C. Each graph plots α as a function of A over the range $10^{-5} \leq A \leq 1$ for a

range of C values ($C=0.0001$, 0.001 , and 0.01); each graph was also prepared using a different B value ($B=0.001$, 0.1 , 1 , and 10). These ranges of values were selected based on consideration of the discussion of reasonable ranges of primary inputs given in Section 4. In the following discussion, mathematical analysis supported by these graphs is used to determine the dependence of α on the primary inputs.

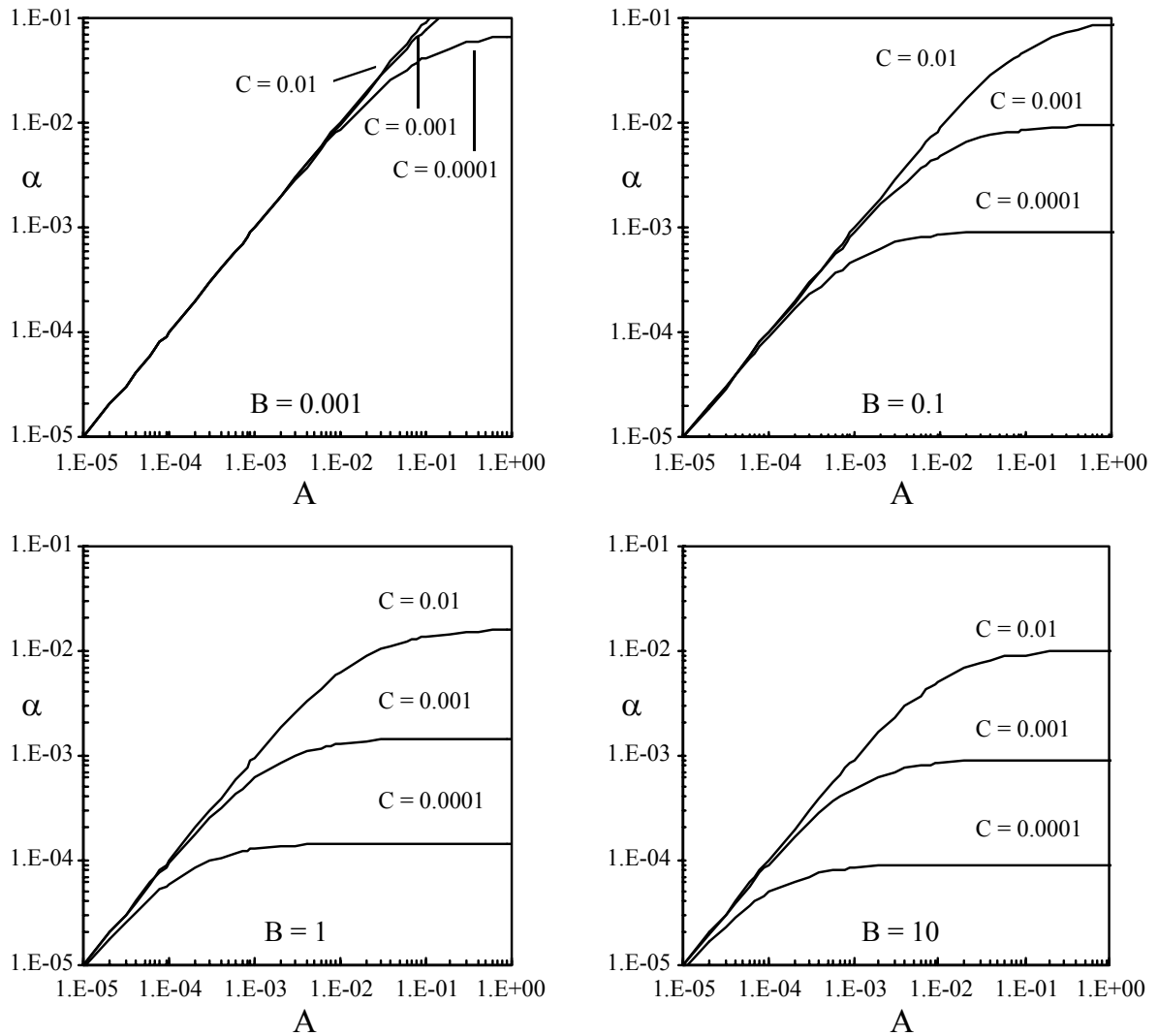


Figure A1. Variation in α with changes in the parameters A, B, and C.

Thus, the $B=0.001$ plot corresponds to the case where diffusion is the dominant transport mechanism through the foundation. Mathematically, when $B < 0.1$, Equation (A1) can be approximated by:

$$\alpha = \frac{[A]}{1 + [A] + \left[\frac{A}{C}\right](B)}, \quad B < 0.1 \quad (\text{A4})$$

Provided that $(AB/C) < 0.1$, it is expected that α should vary only with A:

$$\alpha = \frac{[A]}{1 + [A]}, \quad B < 0.1 \text{ and } \frac{AB}{C} < 0.1 \quad (\text{A5})$$

This behavior is seen with decreasing A in the $B=0.001$ and $B=0.1$ plots (note that $\alpha=A$ for $A \ll 1$). Physically, this condition ($B < 0.1$ and $AB/C < 0.1$) corresponds to cases where diffusion through soil is the overall rate-limiting transport mechanism. Consequently, α varies only with changes in A, so that D_T^{eff} , A_B , Q_B , and L_T (and any related secondary inputs) are the only critical inputs. The $B=0.001$ curves also show that changes in α with respect to changes in D_T^{eff} , A_B , Q_B , and L_T are at most linear (e.g., increasing L_T by a factor of two decreases α by 1/2, increasing D_T^{eff} by a factor of two increases α by a factor 2).

If $B < 0.1$ and $(AB/C) > 10(1+A)$, then:

$$\alpha = \frac{[C]}{[B]}, \quad B < 0.1 \text{ and } \frac{AB}{C} > 10(1+A) \quad (\text{A6})$$

This behavior is seen in the asymptotes of the $B=0.1$ curves as A increases. Physically, this condition ($B < 0.1$ and $AB/C > 10(1+A)$) corresponds to cases where diffusion through the foundation is the overall rate-limiting transport mechanism. Under these conditions α varies only with changes in the ratio (C/B) , so that $D_{\text{crack}}^{\text{eff}}$, A_B , Q_B , η , and L_{crack} (and any related secondary inputs) are the only critical inputs. The $B=0.1$ curves also show that changes in α with respect to changes in these parameters are at most linear.

The B=10 plot corresponds to the case where advection is the dominant transport mechanism across the foundation. Mathematically, when $B > 3$, then $\exp(B) > 10$ and Equation (A1) reduces to:

$$\alpha = \frac{[A]}{1 + \left[\frac{A}{C}\right]}, \quad B > 3 \quad (\text{A7})$$

Therefore, α is expected to be independent of B for $B > 3$, and this can be seen by comparing the curves in the B=1 and B=10 plots. The vapor attenuation coefficient α is dependent only on those inputs affecting the values of A and C. Thus, L^{crack} , $D_{\text{crack}}^{\text{eff}}$, and η are non-critical inputs under these conditions. Again, the B=1 and B=10 graphs show that the sensitivity of α to changes in the primary inputs appearing in A and C is at most linear, and under the conditions discussed below, some other inputs may also be non-critical.

If in addition to the condition $B > 3$, advective transport across the building foundation is the overall limiting transport mechanism between the point of interest (L_T) and the enclosed space, then $(A/C) > 10$ and:

$$\alpha = C, \quad B > 3 \quad \text{and} \quad \frac{A}{C} > 10 \quad (\text{A8})$$

This limit is observed in Figure A1 as all α -vs-A curves asymptote with increasing A to $\alpha=C$ for B=1 and B=10. This condition is most likely to be met when assessing the attenuation between soil gas immediately below a foundation and indoor air ($L_T \rightarrow 0$). Under these conditions, we need only know Q_{soil} and Q_B (or the ratio Q_{soil}/Q_B) to estimate α . Sensitivity of α to changes in Q_{soil} and Q_B is linear in Equation (A8).

If $B > 3$ and transport through the vadose zone is the limiting transport mechanism between the point of interest (L_T) and the enclosed space, then $(A/C) < 0.1$, and:

$$\alpha = A, \quad B > 3 \quad \text{and} \quad \frac{A}{C} < 0.1 \quad (\text{A9})$$

This limit is observed in Figure A1 as all α -vs-A curves asymptote with decreasing A to $\alpha=A$ for B=1 and B=10. This condition is most likely to be met when we are interested in assessing the

attenuation between soil gas located more than a few meters below a foundation, or possibly the attenuation of vapors originating from dissolved groundwater contamination. Under these conditions, we need only know D_T^{eff} , A_B , Q_B , and L_T to estimate α .

Basic Nomenclature

- A, B, C = dimensionless parameters defined in Equations (5), (A2) and (A3)
 A_B = the surface area of the enclosed space in contact with soil [m^2]
 α = $(C_{\text{indoor}}/C_{\text{source}})$; C_{indoor} denotes the indoor air concentration and C_{source} is the vapor concentration at some depth (both in consistent units)
 C_{indoor} = the indoor air concentration [mg/m^3]
 C_{source} = the vapor concentration at some depth, or the vapor concentration calculated to be in equilibrium with contaminated groundwater [mg/m^3]
 D^{eff} = the effective overall vapor-phase diffusion coefficient [m^2/d]
 $D_{\text{crack}}^{\text{eff}}$ = the effective overall vapor-phase diffusion coefficient through the walls and foundation cracks [m^2/d]
 D_T^{eff} = the effective overall vapor-phase diffusion coefficient between the foundation and the depth L_T [m^2/d]
 E_B = the building air exchange rate [d^{-1}]
 η = the fraction of enclosed space surface area open for vapor intrusion [m^2/m^2]; this is sometimes referred to as the “crack factor” and is estimated to be the total area of cracks, seams, and any perforations of surfaces in contact with soil divided by the total area in contact with soil.
 L_{crack} = the enclosed space foundation thickness [m]
 L_T = the distance (depth) to the vapor source or other point of interest below foundation [m]
 L_i = thickness of soil layer i [m]
 Q_B = the enclosed space volumetric air flow rate [m^3/d]; usually estimated to be the product of the enclosed-space volume (V_B [m^3]) and the indoor air exchange rate (E_B [$1/d$])
 Q_{soil} = the pressure-driven soil gas flow rate from the subsurface into the enclosed space [m^3/d]
 V_B = the enclosed space volume (i.e., the volume of the basement or first floor room of a slab-on-grade construction) [m^3]

NOTE

API publications may be used by anyone desiring to do so. Every effort has been made by the Institute to assure the accuracy and reliability of the data contained in them; however, the Institute makes no representation, warranty, or guarantee in connection with this publication and hereby expressly disclaims any liability or responsibility for loss or damage resulting from its use or for the violation of any federal, state, or municipal regulation with which this publication may conflict.